JCTC Journal of Chemical Theory and Computation

What Active Space Adequately Describes Oxygen Activation by a Late Transition Metal? CASPT2 and RASPT2 Applied to Intermediates from the Reaction of O_2 with a Cu(I)-α-Ketocarboxylate

Stefan M. Huber,[†] Abdul Rehaman Moughal Shahi,[†] Francesco Aquilante,[†] Christopher J. Cramer,*[,‡] and Laura Gagliardi*[,†,‡]

Department of Physical Chemistry, University of Geneva, 30, Quai Ernest Ansermet, 1211 Genève, Switzerland and Department of Chemistry and Supercomputing Institute, University of Minnesota, 207 Pleasant Street SE, Minneapolis, Minnesota 55455-0431

Received June 3, 2009

Abstract: Multiconfigurational second-order perturbation theory calculations based on a complete active space reference wave function (CASPT2), employing active spaces of increasing size, are well converged at the level of 12 electrons in 12 orbitals for the singlet−triplet state−energy splittings of three supported copper−dioxygen and two supported copper−oxo complexes. Corresponding calculations using the restricted active space approach (RASPT2) offer similar accuracy with a significantly reduced computational overhead provided an inner (2,2) complete active space is included in the overall RAS space in order to account for strong biradical character in most of the compounds. The effects of the different active space choices and the outer RAS space excitations are examined, and conclusions are drawn with respect to the general applicability of the RASPT2 protocol.

Introduction

In order to better understand the mechanistic details of substrate oxidations catalyzed by copper-containing metalloenzymes, considerable effort has been devoted to the synthesis and the characterization of smaller copper coordination complexes capable of activating molecular oxygen.[1−9] In a recent example, Hong et al.[10] reported the preparation, structural characterization, and reactivities of related Cu(I)-α-ketocarboxylate complexes supported by iminopyridine ligands appended with arene substituents positioned so as to be susceptible to intramolecular attack by an activated oxygen species (Scheme 1). Using density functional theory (DFT) and multiconfigurational second-order perturbation theory based on a complete active space reference wave function (CASSCF/CASPT2), the microscopic details of the multistep mechanism for the observed oxidation reaction

Scheme 1

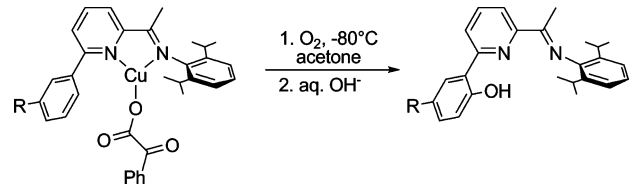

have been elucidated,[10] as has the sensitivity of the reaction path energetics to different ligand sets.[11]

As indicated in Scheme 2 (in which only the N atoms of the supporting ligand are shown), the reaction proceeds by an initial coordination of molecular oxygen to the supported copper complex. Three isomeric structures were predicted at the DFT level, two of which were characterized by end-on coordination of the O_2 moiety, while the other exhibited side-on coordination. Following decarboxylation and subsequent cleavage of the O−O bond in an intermediate peroxybenzoate complex, two isomeric Cu(II)−oxyl species could be accessed, differing in the coordination geometry about the Cu center (square-planar (SP) vs trigonal-bipyra-

* Corresponding authors: E-mail: cramer@umn.edu and laura.gagliardi@unige.ch.

[†] University of Geneva.

[‡] University of Minnesota.

10.1021/ct900282m CCC: $40.75
Published on Web 10/06/2009

Scheme 2

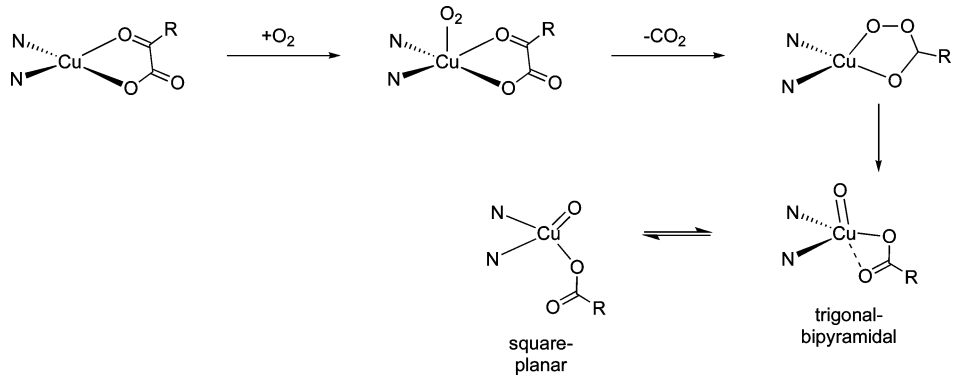

midal (TBP); the literature alternatively sometimes refers to such species as formal Cu(III)−oxo complexes, but calculations make clear that a Cu(II)−oxyl formulation is more appropriate given the relevant electronic structures).[10,12−15] Both the peroxybenzoate and the Cu(II)-oxyl intermediates were determined to be highly reactive with respect to the oxidation of the pendant arene ring in the iminopyridine ligand. Experimental investigations designed to isolate a Cu(II)-oxyl intermediate and to extend the reactivity of such species to external substrates continue to be actively pursued.

Considering in more detail the theoretical modeling of these species, several key intermediates are well described as having biradical character. In particular, the initial oxygen adducts and the Cu(II)-oxyl intermediates. In the case of the oxygen adducts, whether viewed as complexes of molecular O_2 with Cu(I) or as Cu(II)-superoxide compounds, two electrons are effectively localized on distinct centers: the two O atoms in the former instance and the Cu(II) and one O atom in the latter.[16] The latter localization also prevails in the Cu(II)-oxyl intermediates. Such biradical character introduces challenges with respect to computing the properties of singlet electronic states based on single-determinant formalisms, like Kohn−Sham density functional theory (KS-DFT).[17] A proper spin and spatial wave function for a biradical singlet, also sometimes referred to as an open-shell singlet, formally requires a minimum of two determinants. Nevertheless, by invocation of a relationship between the eigenvalues of the Heisenberg−Slater−Dirac Hamiltonian[18−21] and the energies obtained from broken-symmetry and high-spin single-determinant calculations,[22−25] DFT models have been successfully employed to compute state−energy splittings in many open-shell coordination compounds.[9,26−28]

However, this practical approach has a number of drawbacks, particularly insofar as no spin-pure wave function (or density) can be represented by a single determinant for states other than that of the highest spin. Instead, the broken-symmetry states having S_z values below the S_{max} value for the high spin state may be said to be spin contaminated, and as such it is not clear how to evaluate properties *other* than the state energies. To be more precise, we should say that it is the Kohn−Sham determinant that is spin contaminated — the wave function for the corresponding density is not known, so we cannot rigorously assess its spin expectation value, but, in practice, properties determined from broken-symmetry DFT calculations do appear to suffer from spin contamination.

In contrast to single determinantal KS-DFT, multideterminantal states *are* properly represented in multiconfigurational self-consistent field (MCSCF) theory.[29] The complete active space (CASSCF)[30] implementation of this theory constructs a wave function as a linear combination of all possible spin and spatially adapted determinants that may be formed from the distribution of a given number of "active" electrons in a given number of orbitals. The "active space" orbitals are typically chosen based on chemical analysis of the problem at hand, e.g., all bonding and antibonding orbitals associated with one or more bond-making or -breaking processes along a reaction coordinate. When supplemented by multireference second-order perturbation theory, CASSCF/CASPT2,[31] in order to account for dynamical electron correlation effects not included at the CASSCF level, accuracies on the order of 0.2 eV have been documented for state−energy splittings in molecules containing elements throughout the periodic table.[32−41] In the particular case of the copper chemistry discussed above, Hong et al.[10] and Huber et al.[11] compared CASSCF/CASPT2 singlet−triplet splittings to those derived from broken-symmetry DFT calculations in order to assess the likely accuracy of the latter. The two models were in generally good agreement for the Cu(II)-oxyl species, but agreement was not as good for the initial oxygen adducts.

While such comparisons between broken-symmetry DFT and CASSCF/CASPT2 can be informative, the number of determinants in the CASSCF model increases factorially with an increasing number of orbitals in the active space, leading to a practical limit of roughly 16 electrons in 16 orbitals.[17,42] When larger active spaces are needed, e.g., in a trinuclear transition metal complex where a balanced active space might require three sets of valence d and s orbitals, the CASSCF/CASPT2 model cannot be applied in a practical fashion. In order to address this limitation, Malmqvist et al.[43] recently developed a second-order perturbation theory based on the restricted active space self-consistent field method, namely, RASSCF/RASPT2. By subdividing the active space orbitals into three sets, one set entirely equivalent to a CAS space, one set consisting of occupied orbitals *from which* only a limited number of electrons may be excited, and one set consisting of virtual orbitals *into which* only a limited number of electrons may be excited; the number of orbitals and electrons that may be considered is substantially increased relative to the CASSCF/CASPT2 model. While initial results

Scheme 3

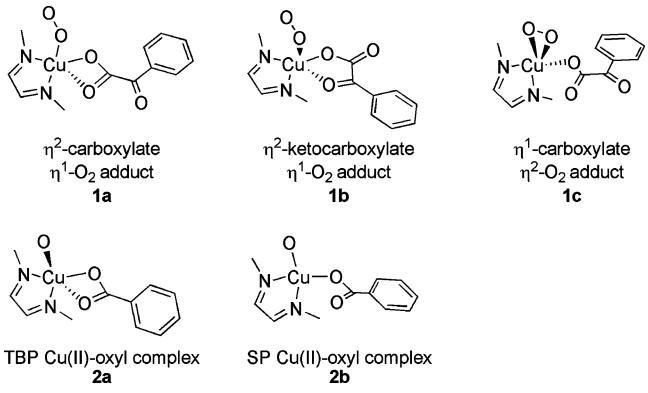

from studies of mono- and binuclear copper−oxygen adducts have been promising, much remains to be learned with respect to the question of how best to choose a RASSCF active space and excitation protocol. The aim of the present paper is to explore this question for biradical copper−oxygen adducts and Cu(II)-oxyl intermediates analogous to those already discussed above. In particular, we examine the predicted singlet−triplet splittings and the relative isomer energies for the three adducts **1a**−**c** and the two intermediates **2a** and **2b** shown in Scheme 3. In order to facilitate this benchmarking study, the sterically demanding N-donor ligand shown in Scheme 1 is replaced by a simplified diimine ligand similarly characterized by two sp^2-hybridized donor nitrogen atoms. We begin with a discussion of the computational details, then present results designed to assess convergence in predicted energies with respect to methodological choices, and conclude with some general observations likely to prove useful in future applications of the RASSCF/RASPT2 model.

Computational Details

Geometries of the structures in Scheme 3 were optimized at the M06-L[44] level of density functional theory adopting a broken-symmetry unrestricted formalism for the nominal singlet states. As we are interested here in comparing different RASSCF/RASPT2 protocols for given geometries, the choice of any particular geometry is arbitrary, but it is perhaps worth emphasizing that computed state−energy splittings in this work are vertical and not adiabatic. Geometry optimizations employed the Cu basis set and pseudopotential of Dolg et al.[45] augmented with three f functions having exponents of 5.10, 1.275, and 0.32; the 6-31G(d) basis set[46] was used for all other atoms.

Multiconfigurational calculations were accomplished according to a number of different protocols. In all cases, basis sets of atomic natural orbital (ANO) and ANO-RCC (for Cu) type[47,48] were employed using contractions of 5s3p2d1f, 3s2p1d, 3s2p1d, 3s2p, and 1s for Cu, O, N, C, and H, respectively. In prior work on the experimentally characterized system of Hong et al., (12,12) CAS spaces were adopted for CASSCF/CASPT2 calculations on the various species with the orbitals included based on a careful assessment of occupation numbers for different active space constructions.[10] These spaces inevitably contained orbitals formed from the bonding and the antibonding combinations of O 2p orbitals and Cu 3d orbitals, with the precise number of σ, π, and nonbonding orbitals being dictated by the chemical structure. The size of the active space was chosen based on consideration of 12 intermediate- and transition-state structures along the reaction coordinate for the overall reaction indicated in Scheme 1. Our goal was to find an active space size that was consistent for all structures and well converged for the predicted singlet−triplet energy splittings. The (12,12) space fulfilled these criteria. With respect to convergence issue, calculations employing expanded (14,14) active spaces predicted very similar singlet−triplet splittings, e.g., 2.33 and 2.34 kcal/mol for structure **1b** of the present study with (12,12) and (14,14) active spaces, respectively.

Those CAS(12,12) active space orbitals most relevant to the present study are illustrated in Figures 1 and 2; in particular, for each of the five structures discussed in this paper, two orbitals in the relevant active space had occupation numbers in the singlet state differing substantially from 2.0 or 0.0, which is consistent with varying degrees of biradical character and are shown in Figure 1. In addition, for the particular case of **1a**, the remaining 10 orbitals are shown in Figure 2. These orbitals are roughly representative of the analogous ones used for the various other structures, which, in the interest of brevity, are not depicted here. For **1a**−**c**, the orbitals in Figure 1 involve π bonding and antibonding combinations of a Cu 3d orbital and an O_2 π^* orbital, and the CAS(12,12) occupation numbers were 1.30, 0.70 (**1a**), 1.05, 0.95 (**1b**), and 1.78, 0.25 (**1c**). In the cases of **2a** and **b**, it was hybrid π orbitals from the Cu 3d and the O 2p orbitals that had occupation numbers of 1.16, 0.85 (**2a**) and 1.11, 0.89 (**2b**). All of these orbitals had occupation numbers of 1.0 in the corresponding triplet states. The other orbitals of the (12,12) active space included all remaining Cu 3d orbitals and a second shell of Cu d orbitals for correlation. When forming smaller (10,10) and (8,8) active spaces, as described below, hybrid orbitals having substantial Cu d character were sequentially removed based on the degree to which their occupation numbers were very near 2.0 or 0.0 for occupied and virtual orbitals, respectively.

In the RASSCF model, the active subspace is divided into three distinct regions: RAS1, RAS2, and RAS3. The RAS2 region is identical to the active region in a CASSCF calculation, i.e., all possible spin- and symmetry-adapted configuration state functions (CSFs) that can be constructed from the orbitals in RAS2 are included in the multiconfigurational wave function. The RAS1 and RAS3 spaces, on the other hand, permit the generation of additional CSFs subject to the restriction that a maximum number of excitations may occur from RAS1, which otherwise contains only doubly occupied orbitals, and a maximum number of excitations may occur into RAS3, which otherwise contains only external orbitals. There are various ways in which one can select the orbitals. In the present case, the maximum size of the full active space was kept at 12 orbitals, in analogy with the CASSCF calculations. Only the two orbitals with an occupation number significantly different from two and zero (see above) were placed in RAS2, with the remaining occupied 3d orbitals (mostly) being in RAS1 orbitals) and the unoccupied 4d orbitals (mostly) being in RAS3. Several levels of maximum excitation

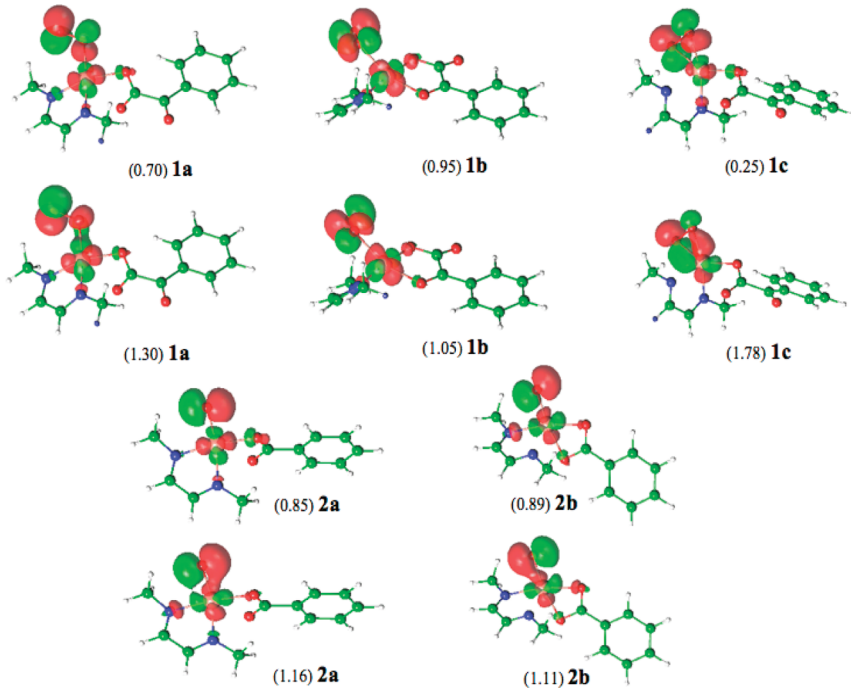

Figure 1. Isodensity surfaces (0.04 au) and occupation numbers for the two active space orbitals with occupation numbers closest to 1.0 from CAS(12,12) calculations for **1a**−**c** and **2a** and **b**. Pairs of orbitals are ordered above and below one another (see also Scheme 3 for isomer ordering). Atomic colors are white (H), green (C), blue (N), red (O), and bronze (Cu).

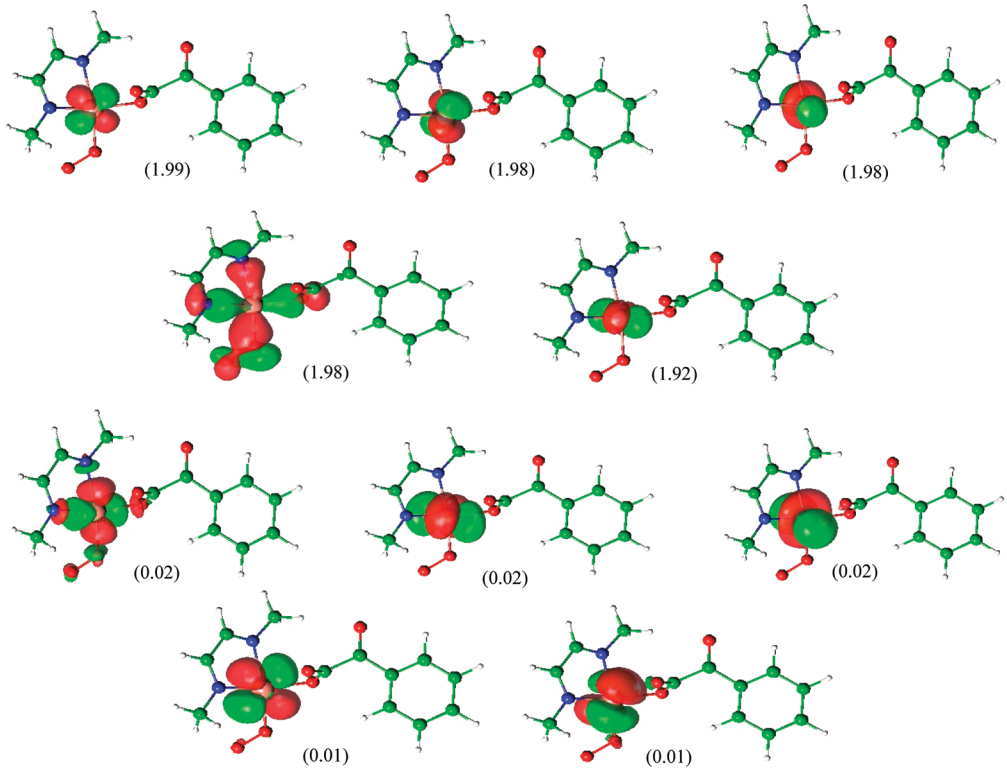

Figure 2. Isodensity surfaces (0.04 au) and occupation numbers for the remaining 10 active space orbitals that are not shown in Figure 1 from a CAS(12,12) calculation for **1a**. Atomic colors are white (H), green (C), blue (N), red (O), and bronze (Cu).

from RAS1 or into RAS3 were considered, namely up to double (SD), triple (SDT), and quadruple excitations (SDTQ). The general notation for a RASPT2 calculation is RASPT2(*j*,*k*)/(*l*,*m*)/*n*, where *j* is the number of electrons in RAS1 and RAS2, *k* is the number of orbitals in all RAS spaces, *l* is the number of electrons in RAS2, *m* is the number of orbitals in RAS2, and *n* is the maximum level of excitation permitted out of RAS1 and into RAS3. Thus, for instance, a RASPT2(12,12)/(2,2)/3 calculation would have 10 electrons and five orbitals in RAS1, two electrons and two orbitals in RAS2, five orbitals in RAS3, and would permit up to triple excitations out of RAS1 or into RAS3.

Table 1. Singlet-Triplet State−Energy Splittings (Kcal/Mol) Predicted at the CASSCF and CASPT2 Levels for Various Active Space Choices

	structure				
active space	**1a**	**1b**	**1c**	**2a**	**2b**
		CASSCF			
(2,2)	0.4	0.4	−4.5	1.8	2.1
(8,8)	−11.7	−13.1	−23.0	−10.7	−10.1
(10,10)	1.8	0.9	−8.8	3.2	3.6
(12,12)	0.8	1.1	−9.4	4.0	4.4
		CASPT2			
(2,2)	−0.1	0.4	−11.7	2.8	3.6
(8,8)	8.1	7.8	−3.9	9.7	10.7
(10,10)	2.5	1.8	−5.4	4.7	5.3
(12,12)	1.2	2.3	−3.1	5.2	6.0

Table 2. Number of Configuration State Functions and Dominant Weights for Various CASSCF Active Space Choices

		dominant CSF weights				
active space	no. CSFs	**1a**	**1b**	**1c**	**2a**	**2b**
(2,2)	3[a]	55/45[b]	51/49	79/21	56/44	54/46
	1	100	100	100	100	100
(8,8)	1 764	59/39	51/48	83/15	61/37	58/40
	2 352	99	99	98	98	98
(10,10)	19 404	59/39	51/47	85/12	57/41	55/43
	29 700	98	98	97	97	97
(12,12)	226 512	63/34	51/46	85/10	56/41	54/43
	382 239	97	97	97	96	96

[a] Singlet above triplet. [b] Singlet above triplet; the weights of the two dominant CSFs are reported in the former case, and the weight of the one dominant CSF in the latter case.

In all calculations, Cholesky decomposition[49,50] of the two electron integrals was accomplished with a threshold of 10^{-5} au. Reduced scaling evaluation of the Fock exchange matrices in the CASSCF and RASSCF calculations was accomplished by means of the local-K (LK) screening approach[51] employing localized Cholesky orbitals.[52]

M06-L calculations were done with MN-GFM,[53] a locally modified version of the Gaussian03 electronic structure program suite.[54] All CASSCF/CASPT2 and RASSCF/RASPT2 calculations were done with the MOLCAS 7.2 package.[42]

Results and Discussion

Singlet−Triplet State−Energy Splittings. We begin with an examination of the predicted singlet−triplet splittings at the CASSCF and RASSCF and the CASPT2 and RASPT2 levels, as a function of active space choice. Results from CASSCF and CASPT2 calculations are presented in Table 1.

A few trends merit discussion in the CASSCF/CASPT2 singlet−triplet splittings. First, at the CASSCF level, expanding the active space from (10,10) to (12,12) causes changes in the predicted splittings of 1 kcal/mol or less. At the CASPT2 level, the same change in active space size has an effect of roughly similar magnitude, with the exception of **1c** where it is a somewhat larger 2.3 kcal/mol. In addition, the change in the splitting going from the CASSCF level to the CASPT2 level is 0.4, 1.2, 6.3, 1.2, and 1.6 kcal/mol, respectively, for **1a**−**c** and **2a** and **b**. Dynamical correlation at the CASPT2 level favors the triplet state in every instance, but the change is small with the exception of **1c**, which continues to be somewhat of an outlier. All of these observations suggest that the CASPT2(12,12) values may be considered to be reasonably well converged (and, as noted in the Computational Details Section, expanding to (14,14) in select instances led to negligible changes in the predicted splittings). Thus, for future discussion purposes, we will consider the CASPT2(12,12) values to be reliable, with the possible exception of **1c**, where a larger uncertainty exists.

With respect to smaller active spaces, it is noteworthy that the very simple (2,2) space offers a reasonable accuracy in most instances, consistent with a fairly simple biradical description for the species under consideration. The exception is again **1c**, but, as can be judged by the occupation numbers of the frontier orbitals for this structure in Figure 1, it is the least biradicaloid of the five compounds considered here, so one would not expect the (2,2) active space to capture as much nondynamical correlation as in the other instances. The (8,8) space leads to very poor predictions at the CASSCF level because it is difficult to find any clear distinction between different (8,8) spaces based on occupation numbers (cf. Figure 2 for the case of **1a**, suggesting that either more or fewer orbitals leads to a better balance). Including additional correlation effects at the CASPT2 level moderates the poor balance of the (8,8) spaces to some extent, but results remain poor compared to CASPT2(12,12).

To put into a better perspective the efficiencies of different active spaces and the biradical characters of the singlet wave functions, we list in Table 2 the numbers of CSFs and the dominant CSF weights for different active space choices. As the numbers of CSFs in the (2,2) spaces are about 5 orders of magnitude fewer than in the (12,12) spaces, the reasonable accuracy of the (2,2) predictions is certainly noteworthy from an efficiency standpoint. Inspection of the CSF weights makes clear that all triplets are essentially single determinantal, while most singlets have very high biradical character (defined as having roughly equal weights of the two dominant configurations), with **1c** being the least biradical.

Turning next to the RASSCF and RASPT2 calculations, Table 3 lists the computed state−energy splittings for various RAS protocols, and Table 4 provides information on the numbers of CSFs and the weights of the dominant configurations associated with different active space choices. For convenience, in Table 3 the results from CASPT2(2,2) and CASPT2(12,12) calculations are recapitulated, and the same is true for CAS(12,12) in Table 4.

The first point to address is the very good performance of the RASPT2(12,12)/(2,2)/2 protocol. Compared to CASPT2-(12,12), all state−energy splittings are predicted to within a mean unsigned error of 0.8 kcal/mol and a maximum unsigned error of 1.1 kcal/mol. Note in particular, that this is a better accuracy than that of CASPT2(2,2), suggesting that the additional excitations considered in the RAS protocol are important. With respect to dynamical correlation energy, the difference between the RASPT2(12,12)/(2,2)/2 and RASSCF(12,12)/(2,2)/2 state−energy splittings is usually small (except for **1c**, it does not exceed 1.2 kcal/mol), but

Table 3. Singlet-Triplet State−Energy Splittings (kcal/mol) Predicted at the RASSCF and RASPT2 levels for Various Active Space Choices

	structure				
active space	**1a**	**1b**	**1c**	**2a**	**2b**
		RASSCF			
(12,12)/(2,2)/2	0.7	0.9	−7.7	3.4	3.8
(12,12)/(2,2)/3	0.8	1.0	−8.5	3.8	4.2
(12,12)/(2,2)/4	0.8	1.1	−9.2	3.9	4.4
(12,12)//2[a]	24.4	20.4	5.5	32.1	32.6
(12,12)//3[a]	11.7	12.2	−4.7	17.8	14.7
		RASPT2			
(12,12)/(2,2)/2	0.8	1.5	−2.6	4.1	5.0
(12,12)/(2,2)/3	0.8	1.9	−2.1	4.8	5.8
(12,12)/(2,2)/4	1.6	2.3	2.0	5.3	6.0
(12,12)//2[a]	22.9	25.6	5.3	25.8	25.4
(12,12)//3[a]	2.3	3.0	−5.9	17.5	9.4
		CASPT2			
(2,2)	−0.1	0.4	−11.7	2.8	3.6
(12,12)	1.2	2.3	−3.1	5.2	6.0

[a] The excitation level for the triplet state is formally one higher, since the generation of a triplet state from the starting set of six occupied RAS1 and six virtual RAS3 orbitals requires an initial single excitation.

Table 4. Number of Configuration State Functions and Dominant Weights for Various Rasscf Active Space Choices and Excitation Levels

		dominant CSF weights				
active space	no. CSFs	**1a**	**1b**	**1c**	**2a**	**2b**
(12,12)/(2,2)/2	2 028[a]	60/37[b]	51/46	84/13	56/41	54/43
	2 891	97	97	97	97	96
(12,12)/(2,2)/3	14 428	57/31	47/41	77/10	51/37	49/39
	22 991	88	88	87	87	87
(12,12)/(2,2)/4	54 678	62/33	51/44	84/9	55/40	53/42
	91 091	95	95	95	94	94
(12,12)//2[c]	703	90/−[d]	90/−[d]	89/6	82/15	84/13
	8 991	97	97	97	97	97
(12,12)//3[c]	6 003	66/15	67/13	65/31	59/22	56/24
	45 441	90	88	88	82	88
CAS(12,12)	226 512	63/34	51/46	85/10	56/41	54/43
	382 239	97	97	97	96	96

[a] Singlet above triplet. [b] Singlet above triplet; the weights of the two dominant CSFs are reported in the former case, and the weight of the one dominant CSF in the latter case. [c] The excitation level for the triplet state is formally one higher, since the generation of a triplet state from the starting set of six occupied RAS1 and six virtual RAS3 orbitals requires an initial single excitation. [d] No second singlet CSF has a weight of 5% or higher.

the RASPT2 model is in better agreement with CASPT2(12,12) in every instance, indicating the utility of the post-RASSCF PT2 calculation. Considering, as indicated in Table 4, that the number of CSFs is reduced by about 2 orders of magnitude on going from CASPT2(12,12) to RASPT2(12,12)/(2,2)/2, this is a particularly impressive level of accuracy.

As an additional measure of the importance of the orbital relaxation associated with RASSCF excitations outside the central (2,2) CAS space, we examined using the orbitals from a CASSCF(2,2) calculation as *frozen* orbitals for a subsequent RASPT2(12,12)/(2,2)/2 calculation. That is, we did *not* reoptimize any molecular orbital coefficients after the CAS(2,2) step but instead only optimized the configuration interaction coefficients in the RAS(12,12)/(2,2)/2 wave function that was used as the multiconfigurational reference for the PT2. Such a calculation is computationally very inexpensive. However, the results were essentially the same as those obtained at the CASPT2(2,2) level, indicating that orbital relaxations associated with the RAS outer space excitations do improve the agreement with CASPT2 calculations using larger active spaces.

Turning to the consideration of triple and quadruple excitations in the outer RAS spaces, changes in predicted state−energy splittings tend to be small but offer quantitative improvement in the agreement with CASPT2(12,12) values. At the RASPT2(12,12)/(2,2)/4 level, for which the number of CSFs is reduced by a factor somewhat larger than 4 compared to the CASPT2(12,12) level, the agreement averages within 0.1 kcal/mol for all structures other than **1c**. For this latter structure, higher RAS excitations lead to progressively worse agreement with CASPT2(12,12). As already noted above, this structure is the one case where the (12,12) active space may not represent a sufficiently large space to be considered converged, and thus, it may not be as meaningful to make a comparison for this least biradicaloid dioxo species. As a technical note, the current implementation of the RASPT2 model in MOLCAS is such that RASSCF convergence tends to be rapid when only double excitations are considered and slows down considerably when higher levels of excitations are allowed. While future development efforts will be targeted to improve the convergence in the latter instance, the excellent accuracy of the RASPT2(12,12)/(2,2)/2 model for the present test set bodes well for future applications to other analogous biradicaloid transition-metal oxo species.

A curious feature of the outer-space RAS excitations that merits further study is the degree to which dominant configuration weights are reduced when excitations are limited to no more than triples. As seen in Table 4, in every instance the dominant configuration weights drop by 3−10% at the RASSCF(12,12)/(2,2)/3 level compared to that of the RASSCF(12,12)/(2,2)/2 level. Of course, one might argue that as the number of possible CSFs increases to the full CI limit, one might naturally expect the weights of the individual configurations to drop somewhat, but on going to the RASSCF(12,12)/(2,2)/4 level, i.e., including quadruples, the weights return to very near the RASSCF(12,12)/(2,2)/2 values and are moreover almost identical to the CASSCF(12,12) values. Such oscillating behavior among the even and the odd levels of excitations is reminiscent of the convergence behavior of the correlation energy in the Møller−Plesset perturbation theory explored in detail by Olsen et al.[55,56] and also by Luna et al.[57] This last reference[57] deserves special attention since it focuses on the problem of poor convergence with second-order perturbation theory for ground-state Cu(I) complexes.

In order to study this point further, one would have to monitor CSF weights for still higher levels of excitation. For the present molecules, however, such calculations are prohibitively expensive. We will investigate this behavior for smaller test systems in the future.

We now consider an alternative protocol, which one might adapt in the absence of any knowledge of biradical character in the subject molecules. In particular, we examine RASPT2 protocols with a total of 12 electrons in 12 orbitals without

any inner CAS(2,2) space, permitting up to double the excitations from the occupied to the virtual space. To be precise, it is the singlet state for which excitations up to double are allowed. For the triplet state, generation of a triplet wave function already requires a single excitation (with spin flip), so that the triplet-state calculations actually permit up to triple excitations in order to correspond properly with the singlet analogs. In any case, as shown in Table 3, the accuracy of the RASPT2(12,12)//2 approach is extremely poor, with errors as high as 23 kcal/mol. The direction of the errors indicates that the correlation energies predicted for the singlet states are considerably smaller than those for the triplet states. Inspection of the CSF weights (Table 4) indicates that the problem appears to be with the failure of the RAS(12,12)//2 protocol to adequately relax the orbitals such that the weight of a formally doubly excited configuration becomes fairly close to that of the reference configuration for the biradicaloid singlet states.

In addition to noting that this problem is least severe for **1c**, which is the least biradicaloid of all of the singlets, inspection of the absolute electronic energies further illustrates the importance of this point. Triplet **1a**, for example, has a predicted electronic energy at the CAS(2,2) level of −2 598.57346. At the RAS(12,12)/(2,2)/2 level, the corresponding energy is −2 598.73770, and at the RAS(12,12)//2, it is −2 598.73794; thus, the two are very close, as might be expected. For the singlet state, on the other hand, the CAS(2,2) electronic energy is −2 598.57290, and the RAS(12,12)/(2,2)/2 energy is −2 598.73662, but the RAS(12,12)//2 energy is −2 598.69905, the final value being 37 mE_h more positive than the RAS(12,12)/(2,2)/2 reference. This failure to adequately rotate the most important occupied and virtual orbital(s) in the SCF procedure of the RAS(12,12)//2 calculations will merit further attention but suggests that strong nondynamical correlation effects should still be addressed with inner CASSCF spaces when possible.

The situation improves somewhat when the RASSCF excitation level is increased. Examining the state−energy splittings and the CSF weights for the RASPT2(12,12)//3 level, the former are in reasonable agreement with the CASPT2(12,12) results (except for **2a**) but are not as good as the state−energy splittings predicted at the RASPT2(12,12)/(2,2)/2 level, where fewer CSFs are required. Interestingly, the CSF weights are again depressed upon the inclusion of triple excitations; the amount of that depression for the most dominant CSF in the singlet is coincidentally about equal to the degree to which a single configurational character is overemphasized by the failure to include an interior CASSCF(2,2) space, but consideration of the minor singlet CSF or the dominant triplet CSF clearly illustrates the phenomenon. The trend on going from the RASPT2(12,12)//2 to the RASPT2(12,12)//3 level suggests that good results might be expected from the RASPT2(12,12)//4 level. However, the final level requires formal quintuple excitations to generate quadruply excited triplet states, and we were not successful in converging such calculations, which in any case require a number of CSFs so large that there is little point in not simply carrying out a full CASPT2 calculation.

Table 5. Triplet Energies (kcal/mol) of **1b** and **1c** Relative to **1a** and **2b** Relative to **2a** Computed at Various Levels of Theory

	structure		
theory	**1b**	**1c**	**2b**
	RASPT2		
(12,12)/(2,2)/2	3.9	−12.9	−0.1
(12,12)/(2,2)/3	4.3	−14.0	0.4
(12,12)/(2,2)/4	4.4	−13.3	0.1
(12,12)//2[a]	3.8	−13.4	0.0
(12,12)//3[a]	3.2	−15.1	−2.4
	CASPT2		
(2,2)	2.3	−12.6	1.3
(8,8)	4.2	−12.8	1.2
(10,10)	4.6	−13.6	1.1
(12,12)	4.7	−13.8	1.3
	DFT		
M06-L	1.9	4.4	−0.7

[a] The excitation level for the triplet state is formally one higher, since the generation of a triplet state from the starting set of six occupied RAS1 and six virtual RAS3 orbitals requires an initial single excitation.

Table 6. Singlet Energies (kcal/mol) of **1b** and **1c** relative to **1a** and **2b** relative to **2a** Computed at Various Levels of Theory

	structure		
theory	**1b**	**1c**	**2b**
	RASPT2		
(12,12)/(2,2)/2	4.7	−16.3	−0.9
(12,12)/(2,2)/3	5.4	−16.9	−0.6
(12,12)/(2,2)/4	5.0	−13.0	−0.6
(12,12)//2	6.6	−31.0	0.4
(12,12)//3	3.8	−23.3	5.8
	CASPT2		
(2,2)	2.9	−24.2	0.5
(8,8)	3.9	−24.8	0.1
(10,10)	3.8	−21.5	0.5
(12,12)	5.9	−18.0	0.4

Relative Energies of Different Isomers. In addition to state−energy splittings, we examined the differences in specific spin-state energies for the three dioxygen adducts and the two copper−oxo isomers. These results are presented in Table 5 for the triplet states and Table 6 for the singlet states. As we consider here only a single geometry for each species (see Computational Details Section) and as we have already noted the relative performances of the various models for singlet−triplet energy differences, in principle, the data in Table 6 should be evident from the consideration of Table 5 and the foregoing data, but it is helpful to see where errors cancel or reinforce the isomer energies.

For the triplet states, there is good convergence in the CASPT2 relative energies as the active space is increased from (2,2) to (12,12) in size. Moreover, all of the RASPT2 protocols are in fairly good agreement with the CASPT2(12,12) predictions, with the best agreement given by the RASPT2(12,12)/(2,2)/3 model (the results are very nearly as good at the RASPT2(12,12)/(2,2)/4 level). While this agreement suggests that the RASPT2 approaches are doing as good a job as CASPT2, the latter model itself may not be particularly accurate for the isomer energies. For comparison, we

computed the M06-L relative energies for the same geometries, and these are also listed in Table 5. For the copper−oxo isomerization, the multireference models and M06-L are in fair agreement, while M06-L predicts the **1b**−**a** energy difference to be smaller by about 3 kcal/mol than computed at the multireference levels. Finally, there is a very large discrepancy between the two types of theory for the **1c**−**a** energy difference, with the multireference models predicting the side-on geometry to be much more stable than either end-on copper−oxygen complex and M06-L predicting the opposite.

As for which, if either, level of theory is more likely to be correct, various considerations suggest that the M06-L predictions are likely to be the more trustworthy, at least for the **1c**−**a** energy difference, where the discrepancy is largest. First, the triplets are all well described by single determinants in which instance DFT is generally quite robust for conformational analysis.[17] Second, consideration of a wide range of supported Cu(I)−dioxygen complexes suggests that the particular ligand set employed here would be more likely to favor an end-on coordination geometry to a side-on one.[6,7,16,58] Third, and perhaps most importantly, were **1c** to be as stable as it is predicted to be at the RASPT2 and CASPT2 levels, the activation energy associated with the subsequent decarboxylation step (Scheme 2) would be inconsistent with the experimental kinetics, where the M06-L prediction *is* consistent.[10] (A precise quantification of this point would require more attention to the optimization of the geometries for all relevant states, but the CASPT2/DFT discrepancy of 18.2 kcal/mol listed for **1c** in Table 5 seems well outside the range of energies that might be associated with minor geometric relaxations in the triplet states).

Thus, while we have established that the (12,12) active space is in all cases, with the possible exception of **1c**, adequate to compute converged state−energy splittings, it would appear that it is *not* adequate to compute isomer energies when the active space is not perfectly converged for all structures considered, with **1c** again being the most problematic case. The geometric differences between **2a** and **b** are small enough that even the (12,12) space seems adequate. It would be interesting to examine whether a full valence active space, using a RAS protocol, would give better results, but such calculations remain outside our present capabilities.

With respect to the relative singlet energies, most trends identified for the triplet states remain the same: RASPT2(12,12)/(2,2)/3 shows the best agreement with CASPT2(12,12) with the double and quadruple excitation levels being nearly as good. However, the RASPT2(12,12)//2 and //3 models are less consistent. They are surprisingly good for both **1b** and **2b**, considering that these levels do very poorly for state−energy splittings, suggesting that the failure to capture singlet correlation energy is quite consistent across geometric isomers. The exception is **1c**, where there is a greater sensitivity to the excitation level. In this case, we do not compare to M06-L, as the computation of biradical singlet energies with DFT presents its own set of complications that go beyond our interests in the present work.

Significance. We have compared the CASPT2 and RASPT2 models for the determination of the singlet−triplet state−energy splittings of five intermediates associated with the formation and the reaction of copper−oxo species derived from oxygenation of Cu(I)-α-ketocarboxylate complexes. Based on consideration of several active spaces, we determined that the CASPT2 model was well converged with a (12,12) active space, but that semiquantitative results could be obtained with a minimal (2,2) space in most instances. Certain intermediate active spaces failed to be balanced, e.g., no good (8,8) active space could be identified. At the RASPT2 level, results were quantitatively very accurate (compared to CASPT2(12,12)) when an inner (2,2) CAS space was included in a total (12,12) space. Including up to double excitations in the outer RAS spaces generated 2 orders of magnitude fewer configuration state functions than the full CASPT2(12,12) calculations but provided essentially equivalent accuracy. Adding additional excitations in the outer RAS spaces led to small but systematic improvements in accuracy.

RASPT2 calculations with a (12,12) space that did *not* include an inner (2,2) CAS space were less accurate in their predictions; such calculations suffer from the requirement that triplet states begin as single excitations (with spin flip) from the (12,12) starting configuration, so the number of triplet configuration state functions is artificially inflated when additional excitations are desired to be consistent with singlet state wave functions. While it was not possible to include a sufficient number of excitations with this approach to demonstrate convergence, the trend in going from singles and doubles to singles, doubles, and triples suggests that it *could* be an effective strategy if efficient SCF convergence schemes are developed.

Neither CASPT2 nor similar RASPT2 isomer energies were judged to be especially accurate with (12,12) active spaces. This may reflect a greater demand on active space size for the computation of geometric energy differences in transition-metal complexes, or it may be specific to the systems under consideration here. This issue deserves further study in systems where full-valence active spaces may be accessible.

Overall, the RASPT2 model, when applied with careful attention to the most critical features associated with possible nondynamical correlation, offers an efficient alternative to more demanding CASPT2 calculations with no loss in accuracy. These results seem particularly encouraging for the study of chemical systems having minimal balanced active spaces that are still so large that they are inaccessible to the conventional CASPT2 method.

Acknowledgment. This work was supported by the Swiss and the U.S. National Science Foundation (grants 200020-120007 and CHE-0610183, respectively). S.M.H. thanks the DAAD for a postdoctoral fellowship.

Supporting Information Available: Geometries of all structures together with electronic state energies from various levels of theory. This material is available free of charge via the Internet at http://pubs.acs.org.

References

(1) Solomon, E. I.; Baldwin, M. J.; Lowery, M. D. *Chem. Rev.* **1992**, *92*, 521–542.

(2) Mirica, L. M.; Ottenwaelder, X.; Stack, T. D. P. *Chem. Rev.* **2004**, *104* (2), 1013–1045.

(3) Lewis, E. A.; Tolman, W. B. *Chem. Rev.* **2004**, *104* (2), 1047–1076.

(4) Klinman, J. P. *J. Biol. Chem.* **2006**, *281*, 3013–3016.

(5) Hatcher, L. Q.; Karlin, K. D. *Adv. Inorg. Chem.* **2006**, *58*, 131–184.

(6) Itoh, S. *Curr. Opin. Chem. Biol.* **2006**, *10* (2), 115–122.

(7) Cramer, C. J.; Tolman, W. B. *Acc. Chem. Res.* **2007**, *40* (7), 601–608.

(8) Rolff, M.; Tuczek, F. *Angew. Chem., Int. Ed.* **2008**, *47* (13), 2344–2347.

(9) Gherman, B. F.; Cramer, C. J. *Coord. Chem. Rev.* **2009**, *253*, 723–753.

(10) Hong, S.; Huber, S. M.; Gagliardi, L.; Cramer, C. J.; Tolman, W. B. *J. Am. Chem. Soc.* **2007**, *129* (46), 14190–14192.

(11) Huber, S. M.; Ertem, M. Z.; Aquilante, F.; Gagliardi, L.; Tolman, W. B.; Cramer, C. J. *Chem. Eur. J.* **2009**, *15*, 4886–4895.

(12) Yamaguchi, K.; Takahara, Y.; Fueno, T. In *Applied Quantum Chemistry*; Smith, V. H., Schaefer, H. F., Morokuma, K., Eds. Kluwer: Dordrecht, The Netherlands, 1986; pp 155−184.

(13) Schroder, D.; Holthausen, M. C.; Schwarz, H. *J. Phys. Chem. B* **2004**, *108* (38), 14407–14416.

(14) Decker, A.; Solomon, E. I. *Curr. Opin. Chem. Biol.* **2005**, *9*, 152–163.

(15) Gherman, B. F.; Tolman, W. B.; Cramer, C. J. *J. Comput. Chem.* **2006**, *27* (16), 1950–1961.

(16) Cramer, C. J.; Gour, J. R.; Kinal, A.; Włoch, M.; Piecuch, P.; Moughal Shahi, A. R.; Gagliardi, L. *J. Phys. Chem. A* **2008**, *112* (16), 3754–3767.

(17) Cramer, C. J. *Essentials of Computational Chemistry: Theories and Models*, 2nd ed.; John Wiley & Sons: Chichester, U.K., 2004; pp 385−427.

(18) Heisenberg, W. *Z. Phys.* **1928**, *49*, 619.

(19) Dirac, P. A. M. *Proc. R. Soc. London, Ser. A* **1929**, *123*, 714.

(20) Van Vleck, J. H. *Rev. Mod. Phys.* **1945**, *17*, 27.

(21) Slater, J. C. *Rev. Mod. Phys.* **1953**, *25*, 199.

(22) Ziegler, T.; Rauk, A.; Baerends, E. J. *Theor. Chim. Acta* **1977**, *43*, 261–271.

(23) Noodleman, L. *J. Chem. Phys.* **1981**, *74* (10), 5737–5743.

(24) Yamaguchi, K.; Jensen, F.; Dorigo, A.; Houk, K. N. *Chem. Phys. Lett.* **1988**, *149*, 537–542.

(25) Soda, T.; Kitagawa, Y.; Onishi, T.; Takano, Y.; Shigeta, Y.; Nagao, H.; Yoshioka, Y.; Yamaguchi, K. *Chem. Phys. Lett.* **2000**, *319* (3−4), 223–230.

(26) Ciofini, I.; Daul, C. A. *Coord. Chem. Rev.* **2003**, *238*, 187–209.

(27) Neese, F. *Coord. Chem. Rev.* **2009**, *253*, 526–563.

(28) Harvey, J. N. *Struct. Bonding (Berlin)* **2004**, *112*, 151–183.

(29) Schmidt, M. W.; Gordon, M. S. *Annu. Rev. Phys. Chem.* **1998**, *49*, 233–266.

(30) Roos, B. O.; Taylor, P. R.; Siegbahn, P. E. M. *Chem. Phys.* **1980**, *48*, 157–173.

(31) Andersson, K.; Malmqvist, P.-Å.; Roos, B. O. *J. Chem. Phys.* **1992**, *96* (2), 1218–1226.

(32) Roos, B. O.; Malmqvist, P-Å. *Phys. Chem. Chem. Phys.* **2004**, *6*, 2919–2927.

(33) Azizi, Z.; Roos, B. O.; Veryazov, V. *Phys. Chem. Chem. Phys.* **2006**, *8* (23), 2727–2732.

(34) Gagliardi, L. *J. Am. Chem. Soc.* **2003**, *125*, 7504–7505.

(35) Gagliardi, L.; La Manna, G.; Roos, B. *Faraday Discuss.* **2003**, *124*, 63–68.

(36) Gagliardi, L.; Pyykkö, P. *Angew. Chem., Int. Ed.* **2004**, *43* (12), 1573–1576.

(37) Gagliardi, L.; Pyykkö, P.; Roos, B. O. *Phys. Chem. Chem. Phys.* **2005**, *7*, 2415–2417.

(38) Gagliardi, L.; Cramer, C. J. *Inorg. Chem.* **2006**, *45* (23), 9442–9447.

(39) Roos, B. O.; Gagliardi, L. *Inorg. Chem.* **2006**, *45*, 803–807.

(40) Roos, B. O.; Borin, A. C.; Gagliardi, L. *Angew. Chem., Int. Ed.* **2007**, *46* (9), 1469–1472.

(41) Gagliardi, L.; Roos, B. O. *Chem. Soc. Rev.* **2007**, *36*, 893–903.

(42) Karlström, G.; Lindh, R.; Malmqvist, P.-Å.; Roos, B. O.; Ryde, U.; Veryazov, V.; Widmark, P. O.; Cossi, M.; Schimmelpfennig, B.; Neogrady, P.; Seijo, L. *Comput. Matl. Sci.* **2003**, *28* (2), 222–239.

(43) Malmqvist, P. Å.; Pierloot, K.; Moughal; Shahi, A. R.; Cramer, C. J.; Gagliardi, L. *J. Chem. Phys.* **2008**, *128*, 204109.

(44) Zhao, Y.; Truhlar, D. G. *J. Chem. Phys.* **2006**, *125* (19), 194101.

(45) Dolg, M.; Wedig, U.; Stoll, H.; Preuss, H. *J. Chem. Phys.* **1987**, *86*, 866–872.

(46) Hehre, W. J.; Radom, L.; Schleyer, P. v. R.; Pople, J. A. *Ab Initio Molecular Orbital Theory*; John Wiley & Sons: New York, 1986.

(47) Pierloot, K.; Dumez, B.; Widmark, P.-O.; Roos, B. O. *Theor. Chim. Acta* **1995**, *90*, 87.

(48) Roos, B. O.; Lindh, R.; Malmqvist, P.-Å.; Veryazov, V.; Widmark, P.-O. *J. Phys. Chem. A* **2005**, *109*, 6575–6579.

(49) Aquilante, F.; Malmqvist, P.-A.; Pedersen, T. B.; Ghosh, A.; Roos, B. O. *J. Chem. Theor. Comput.* **2008**, *4*, 694–702.

(50) Aquilante, F.; Pedersen, T. B.; Lindh, R.; Roos, B. O.; de Meras, A. S.; Koch, H. *J. Chem. Phys.* **2008**, *129* (2), 024113−8.

(51) Aquilante, F.; Pedersen, T. B.; Lindh, R. *J. Chem. Phys.* **2007**, *126* (19), 194106–11.

(52) Aquilante, F.; Pedersen, T. B.; de Meras, A. S.; Koch, H. *J. Chem. Phys.* **2006**, *125* (17), 174101–7.

(53) Zhao, Y.; Truhlar, D. G. *MN-GFM*, Version 4.1; University of Minnesota: Minneapolis, MN, 2008.

(54) Frisch, M. J.; Trucks, G. W.; Schlegel, H. B.; Scuseria, G. E.; Robb, M. A.; Cheeseman, J. R.; Montgomery, J. A.; Vreven, T.; Kudin, K. N.; Burant, J. C.; Millam, J. M.; Iyengar, S. S.; Tomasi, J.; Barone, V.; Mennucci, B.; Cossi, M.; Scalmani, G.; Rega, N.; Petersson, G. A.; Nakatsuji, H.; Hada, M.; Ehara, M.; Toyota, K.; Fukuda, R.; Hasegawa, J.; Ishida, M.; Nakajima, T.; Honda, Y.; Kitao, O.; Nakai, H.; Klene, M.;

Li, X.; Knox, J. E.; Hratchian, H. P.; Cross, J. B.; Adamo, C.; Jaramillo, J.; Gomperts, R.; Stratmann, R. E.; Yazyev, O.; Austin, A. J.; Cammi, R.; Pomelli, C.; Ochterski, J. W.; Ayala, P. Y.; Morokuma, K.; Voth, G. A.; Salvador, P.; Dannenberg, J. J.; Zakrzewski, V. G.; Dapprich, S.; Daniels, A. D.; Strain, M. C.; Farkas, O.; Malick, D. K.; Rabuck, A. D.; Raghavachari, K.; Foresman, J. B.; Ortiz, J. V.; Cui, Q.; Baboul, A. G.; Clifford, S.; Cioslowski, J.; Stefanov, B. B.; Liu, G.; Liashenko, A.; Piskorz, P.; Komaromi, I.; Martin, R. L.; Fox, D. J.; Keith, T.; Al-Laham, M. A.; Peng, C. Y.; Nanayakkara, A.; Challacombe, M.; Gill, P. M. W.; Johnson, B.; Chen, W.; Wong, M. W.; Gonzalez, C.; Pople, J. A. *Gaussian 03, Revision D.01*. Gaussian, Inc.: Wallingford, CT, 2004.

(55) Olsen, J.; Christiansen, O.; Koch, H.; Jorgensen, P. *J. Chem. Phys.* **1996**, *105* (12), 5082–5090.

(56) Christiansen, O.; Olsen, J.; Jörgensen, P.; Koch, H.; Malmqvist, P-Å. *Chem. Phys. Lett.* **1996**, *261* (3), 369–378.

(57) Luna, A.; Alcamí, M.; Mó, O.; Yáñez, M. *Chem. Phys. Lett.* **2000**, *320* (1−2), 129–138.

(58) Maiti, D.; Fry, H. C.; Woertink, J. S.; Vance, M. A.; Solomon, E. I.; Karlin, K. D. *J. Am. Chem. Soc.* **2007**, *129* (2), 264–265.

CT900282M